Sputtering of Water Ice Induced by C$_{60}$ Bombardment: Onset of Plume Formation[†]

I. A. Wojciechowski and B. J. Garrison*

Department of Chemistry, 104 Chemistry Building, Penn State University, University Park, Pennsylvania 16802

Received: August 11, 2005; In Final Form: October 6, 2005

The interaction of a 5 keV C$_{60}$ projectile with amorphous water ice is studied using molecular dynamics computer simulations. The energetic C$_{60}$ molecule causes large-scale collisional events in the subsurface region, involving more than 10^4 water molecules in a time of less than 3 ps. The energy deposited in the sample is sufficiently large to turn the ice into a superheated and superdense gas. The gas is expelled into the vacuum, leading to the formation of a flow that manifests itself in the angular and velocity distributions of emitted water molecules.

Introduction

The use of energetic polyatomic cluster ions as desorption probes in secondary ion mass spectrometry (SIMS) is attracting considerable interest for molecular systems.[1,2] A recent overview article[2] addresses many of the attractive features of cluster bombardment, including enhanced yields, decreased damage in the substrate, reduced interface mixing in depth-profiling experiments, and the potential for depth profiling through molecular solids while retaining chemical specificity. Many of the new observations seem anomalous given the underlying physics of motion associated with atomic bombardment of solids. The open question then is whether dynamics associated with cluster bombardment of solids is the same as in atomic bombardment.

The features of the emission process for C$_{60}$ bombardment of Ag{111} have been studied recently in molecular dynamics (MD) computer simulations.[3,4] The collision events in the silver crystal caused by C$_{60}$ projectiles are clearly different from those initiated by isoenergetic Ga atoms. Bombardment of the Ag surface by 15 keV Ga atoms results in a classic collision cascade with 21 Ag atoms ejected on average per incident projectile. A mesoscale motion including formation of a crater with minimal damage in the surroundings, and a yield of 327 atoms was observed for 15 keV C$_{60}$ bombardment. The motion induced by the C$_{60}$ projectile in these simulations suggests that some level of organized flow might be occurring. The limited number of particles ejected, however, makes it difficult to do a detailed analysis. Concurrent with these calculations, experiments of the velocity distributions of ejected Ag monomers and Ag$_2$ dimers suggest the presence of a flow.[5]

The water ice system provides an ideal system for testing the concept of an organized motion or flow due to cluster bombardment. A large emission yield of ∼2400 water molecules was detected to eject from a water ice sample bombarded by 20 keV C$_{60}^+$ ions.[6,7] There is the potential, thus, to analyze the dynamics of the onset of an organized motion due to C$_{60}^+$ bombardment. Molecular solids such as water ice are typical matrixes for the desorption analysis of organic molecules. Another specific interest to particle emission from water ice is connected with studies of icy satellites of giant planets and comets exposed to solar flares and the flux of particles coming from the magnetospheres of the planets.[8]

The purpose of the current work is to delineate the initial stage or onset of motion due to C$_{60}$ bombardment in a system where there is a significant amount of material removed. The possibility of organized motion in such a system can be elucidated. The bombardment of the water ice by energetic C$_{60}$ molecules is modeled via a molecular dynamics technique because this method has been shown to be effective in describing the motion of the atoms in energetic particle bombardment experiments.[9] The MD simulation approach, therefore, is a valuable tool for obtaining insight into the mechanistic picture behind the complex mesoscale motion initiated by an energetic cluster projectile.

Model Details

Organized motion in C$_{60}$ bombardment of solids, if it is a general phenomenon, should occur in a variety of systems that have sufficient ejection yield, regardless of the specifics of the particular system. The model system of choice is water ice, as explained in the Introduction. Because the simulation is computationally intensive and later we intend to investigate ion effects in the ejection yield of water clusters,[10,11] we have chosen to use a model of water that incorporates a 1 M concentration of Na and Cl ions. We acknowledge that the details of dynamics can be different from pure water, but we do not expect any dramatic influence on the physics of the onset of the plume development.

To ensure a correct description of the mesoscale processes caused by a 5 keV C$_{60}$ impact, a large sample is required. Our lowest estimate for the sample size is 30 nm × 30 nm × 16 nm. This sample size was chosen to minimize edge effects on the dynamics resulting in emission of particles. The sample consists of 400 505 water molecules forming an amorphous ice with 3285 Na$^+$ and Cl$^-$ ions incorporated in the sample. The constraint technique RATTLE[12] and the velocity Verlet algorithm, implemented into the MD code as described previously,[13,14] were used to maintain fixed O−H bond lengths in the water molecules as well as to fix an H−O−H bond angle. All the other details of the water−water[13,14] and ion−water[10,11] interaction potentials used in this study were described in earlier publications. The C−C interactions are described using the

* Corresponding author. Phone: 814 863-2103. Fax: 814 863-5319. E-mail: bjg@psu.edu.

reactive empirical bond-order (REBO) intermolecular potential.[15] The interactions of the carbon atoms with oxygen, hydrogen, sodium, and chlorine are described using the purely repulsive Moliére pairwise potential. The projectile C_{60} is aimed along the surface normal. The C_{60} bombardment process is a mesoscale event and is relatively independent of the C_{60} orientation and the aiming point on the surface,[3,4] thus one trajectory is used for this analysis.

The temperature of the sample before the bombardment is set at about 270 K using the Berendsen algorithm.[16] To avoid artifacts connected with the generation of pressure waves under the C_{60} bombardment, special care is undertaken as described in ref 3. First, the system is made sufficiently large such that the main motion leading to ejection is finished before any possible reflection of energy from the boundaries can reach the crater region. Second, we put a stochastic region[17] at 0 K and a rigid layer on the five sides of the crystal. The stochastic layers attenuate the pressure wave energy, suppressing their reflection from the boundaries. The simulations performed in ref 4 for the 20 keV C_{60} bombardment of silver demonstrate that the development of the motion responsible for emission of particles is well-established by a handful of picoseconds, even though the ejection process is not complete for several times that period. Thus, we limit our consideration to 3 ps to investigate the *onset* of plume formation. We extended the simulations until 9 ps to obtain a statistically significant angular distribution of emitted water dimers.

Results and Discussion

Our analysis aims at a description of the dynamical events initiated by the C_{60} projectiles in the water sample. We discuss the process of energy deposition and demonstrate that the interaction of the C_{60} projectile with the water results in a localized region with high energy density. The material expands in an outward direction, resulting in a jetlike expansion of an energized gas from the volume of the dense collision cascade.

The snapshots of the collision of the 5 keV C_{60} projectile with the water ice sample are shown in Figure 1 for the different times. To obtain more quantitative insight in the mesoscale processes, we display contour plots at different times of the average water molecule radial kinetic energy, $E_\perp = m/2(v_x^2 + v_y^2)$, where m is the molecular mass, v_x and v_y are the velocity components parallel to the ice surface (Figure 2a), as well as plots of the axial velocity component, v_z, (Figure 2b). The coloring scheme in Figure 2a is adjusted so that in the gray regions, the molecules have their initial thermal energy. If they have been set in motion due to the collision event, the color follows the blue to pink color chart. The gray regions in Figure 2b correspond to no net upward or downward motion, the blue regions to motion into the substrate, and the yellow/pink regions to motion toward the vacuum.

The fullerene projectile disintegrates upon impact, ejecting a few fast molecules, as seen in the 0.25 and 0.5 ps frames of Figure 1. During this time, all the carbon atoms penetrate on average to a depth of 3−4 nm in the ice. All the C atoms remain in the ice until 1 ps, a time sufficiently long for their energy to be imparted to the water molecules. Figure 2a for 0.25 ps clearly indicates two regions where the molecules have large radial energies. One region coincides with the core of the collision cascade in the sample. The intensive energy exchange between the C atoms and the target molecules occurs here. The second region is right above the surface where there is emission of fast water molecules. In the axial direction (Figure 2b), these same two regions of motion are distinguishable. The region of the
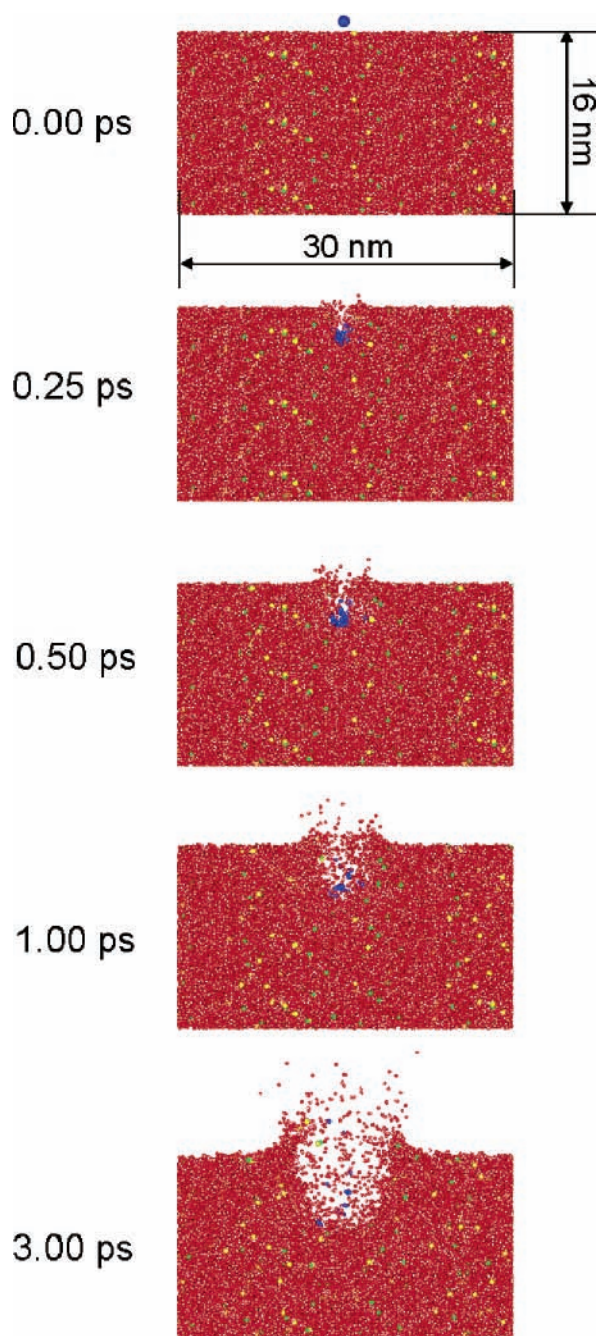

Figure 1. Cross-sectional view of the 5 keV C_{60} interaction with a water sample at different times. Red, blue, green, and yellow spheres represent water molecules, carbon atoms, chloride and sodium ions, correspondingly. Hydrogen atoms are omitted for clarity. Only particles in a 2 nm slice in the center of the crystal are displayed. The impact point is in the center of the surface.

downward motion is associated with the collision cascade of the carbon atoms and the water molecules. Above the surface, the ejected molecules are moving upward toward the vacuum.

At 0.5 ps, there is an energy density of approximately 15 eV/nm^3 in the subsurface region. The region of highest radial kinetic energy goes from the surface to about 5 nm below the surface. About 4×10^3 water molecules are set in motion at this time. The radial kinetic energy is spreading outward, setting more molecules into motion. Even though the radial kinetic energy is spreading outward in an apparent isotropic manner, the axial components of velocity show clear bifurcation. Above approximately 2 nm below the original surface the water molecules are moving upward, coded mainly by the pink color,
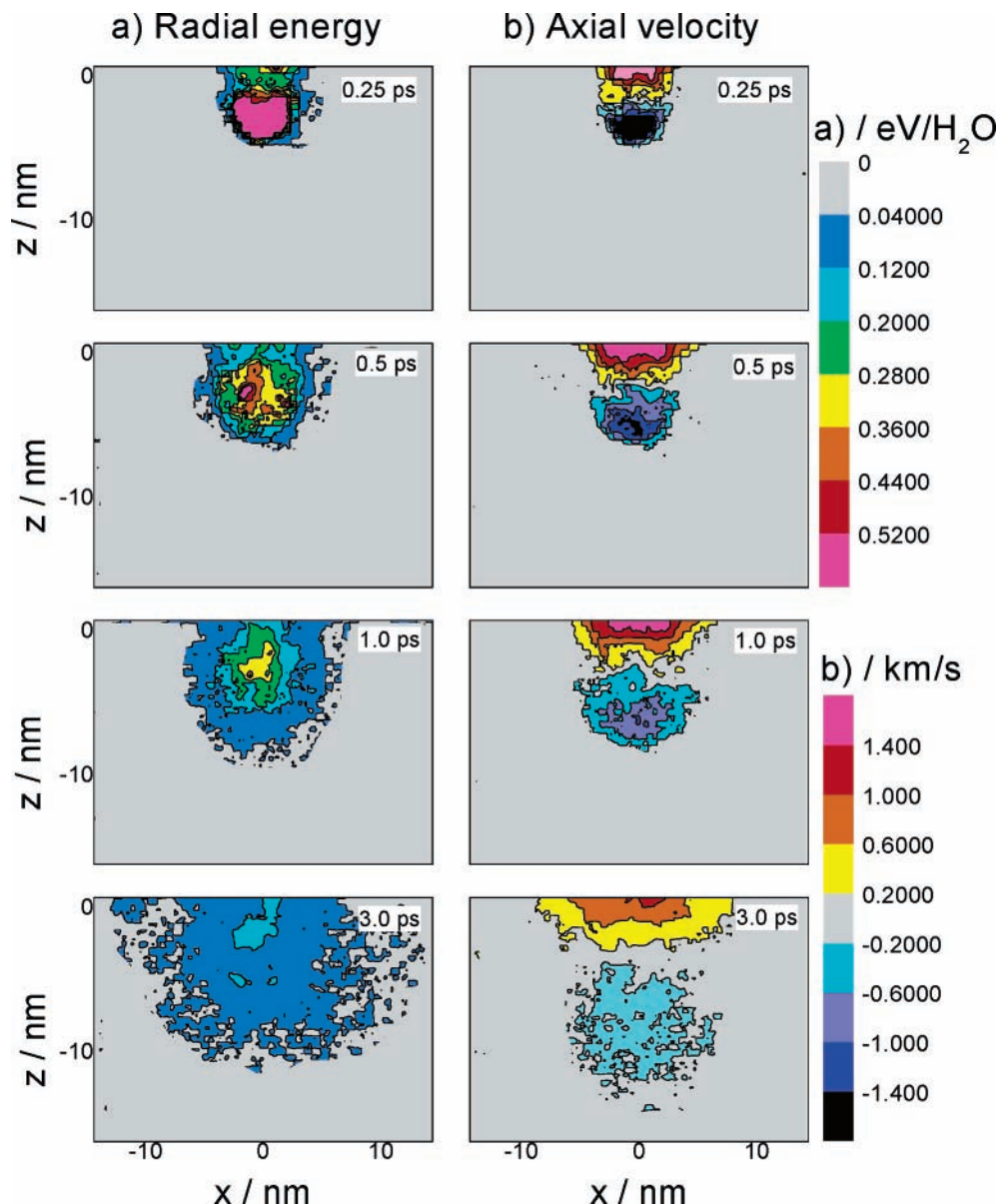
Figure 2. Contour plots for temporal evolution of (a) the radial kinetic energy and (b) the average axial velocity of water molecules in the cells of $0.1 \times 0.1 \times 2.0$ nm^3. The zero ordinate corresponds to the surface position.

in an organized manner. This motion forms as a result the expansion of the superheated gas from the cascade core. Due to the high energy density in the cascade volume, a high pressure builds up and the gas expands quasifreely into the vacuum. This picture resembles an adiabatic gas expansion from the pressurized volume through a nozzle. In addition to the molecules moving toward the vacuum, there is also a region of molecules, denoted by the dark blue color, moving into the substrate.

At 1.0 ps, a crater has clearly started to develop as shown in Figure 1 with the particles ejecting into the vacuum. The energized region, as denoted by the interface between the blue and gray contours in Figure 2a, has an almost spherical shape with the diameter of 9 nm and includes 10^4 molecules. The most energetic region in terms of axial motion is about 2.5 nm deep. This region (coded by orange and yellow colors) represents the clear organized upward flow of the molecules.

The process of gas expelling is developing in time, involving more molecules from the crater walls. The radial energy distribution indicates that a semispherical pressure wave is spreading outward. Even though the system is not at thermal equilibrium, an estimate of a temperature in the energetic region

(blue region of about 10 nm in diameter) is about 700 K, a value that is still well above the critical temperature for water. Thus, the emission of molecules will continue until longer times.

The existence of the upward organized motion should manifest itself in forward peaked angular distributions of the emitted molecules. If the emitted particles go immediately into free flight, they will retain the angular distribution of the source. If a linear cascade or a thermal process is responsible for the particle emission, the angular distribution is of the form cos θ. Collisions between the particles in a dense collision cascade and during the emission as well as flow formation lead to $\sim$cos^n θ, where $n \geq 4$.[18,19] For the time of 9 ps, the total numbers of emitted water monomers, dimers, and trimers are 642, 60, and 21, correspondingly. The larger clusters are represented in amounts less than 10. We can compare, therefore, the angular distributions for water monomers and dimers that are plotted in Figure 3a. The corresponding snapshot of the system is displayed in Figure 3b. The distribution for the monomers is close to cos^4 θ, while the dimers are more strongly forward peaked, as about cos^{20} θ. The difference between the angular distributions of the water monomers and dimers can be easily
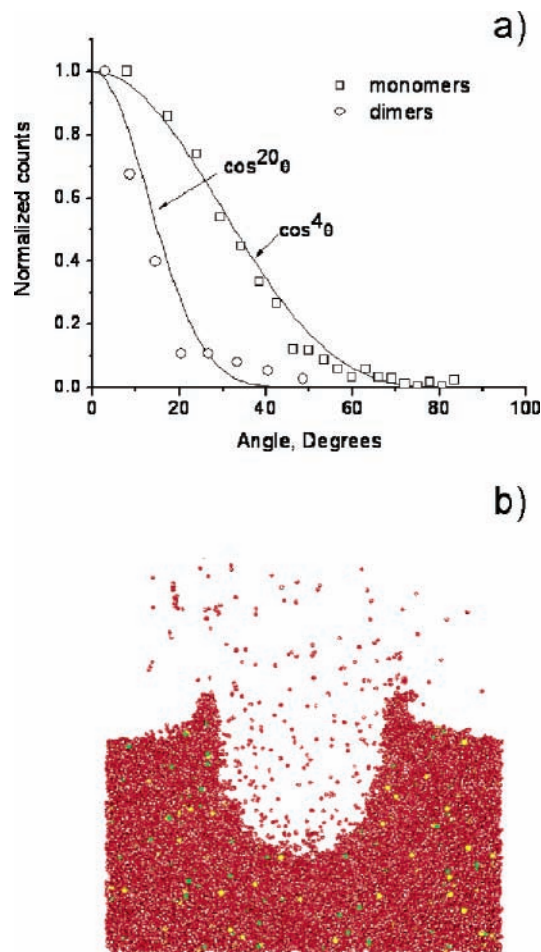
Figure 3. Status of system at 9 ps: (a) angular distributions of water monomers and dimers and (b) cross-sectional view of the system with the same coloring as in Figure 1 except the C atoms are not shown.

understood, if we consider the average axial and radial components of the velocities.[20] In the radial directions, assuming a thermal-like equilibrium, the average velocity should be proportional to the inverse square root of the mass of a particle. In the axial direction, the average velocity should be independent of the particle mass due to the gas expansion in this direction. The axial velocity distributions should be, therefore, similar for water dimers, while the radial distributions should be shifted to lower velocities for larger masses, thus the larger cosine exponent for the dimers. The average radial velocities for water monomers and dimers at 9 ps are estimated to be 1067 and 769 m/s, correspondingly. The ratio of these numbers is very close to $\sqrt{2}$. Average axial velocity components are indeed very close for monomers and dimers, 1750 and 1550 m/s, respectively, being slightly larger for monomers due to a contribution from the fast molecules ejected at early times, as shown in Figure 1.

Conclusion

From the considered plume formation after the impact of a 5 keV C_{60} on a surface of water ice and its temporal evolution

emerge an emission scenario suggested earlier for weakly bonded molecular systems.[21] Energy transferred to the water molecules from the energetic C_{60} randomizes during the first few picoseconds after the impact due to multiple collisions in the dense cascade volume. Due to the high energy density, the average energy of the molecules in the core is sufficient to bring the ice into the state of a superheated and superdense gas. The gas starts to expand into the vacuum through a nozzle-like surface disruption spot, carrying away the energy. The energy outflow to the surroundings also promotes the substrate cooling. The present work establishes a foundation for analyzing dynamics of emission processes due to C_{60} bombardment of molecular solids.

References and Notes

(1) Castner, D. G. *Nature* **2003**, *422*, 129.

(2) Winograd, N. *Anal. Chem.* **2005**, *77*, 143A.

(3) Postawa, Z.; Czerwinski, B.; Szewczyk, M.; Smiley, E. J.; Winograd, N.; Garrison, B. J. *Anal. Chem.* **2003**, *75*, 4402.

(4) Postawa, Z.; Czerwinski, B.; Szewczyk, M.; Smiley, E. J.; Winograd, N.; Garrison, B. J. *J. Phys. Chem. B* **2004**, *108*, 7831.

(5) Sun, S.; Szakal, C.; Winograd, N.; Wucher, A. *J. Am Soc. Mass Spectrom.* **2005**, *16*, 1677.

(6) Wucher, A.; Sun, S.; Szakal, C.; Winograd, N. *Anal. Chem.* **2004**, *76*, 7234.

(7) Szakal, C.; Kozole, J.; Winograd, N. *Appl. Surf. Sci.* Submitted.

(8) Johnson, R. E. *Rev. Mod. Phys.* **1996**, *68*, 305.

(9) Garrison, B. J. In *ToF−SIMS: Surface Analysis by Mass Spectrometry*; Vickerman, J. C., Briggs, D., Eds.; IM Publications and Surface Spectra Limited: Manchester and Chichester, 2001; p 223.

(10) Wojciechowski, I.; Sun, S.; Szakal, C.; Winograd, N.; Garrison, B. J. *J. Chem. Phys. A* **2004**, *108*, 2993.

(11) Wojciechowski, I. A.; Kutliev, U.; Sun, S. X.; Szakal, C.; Winograd, N.; Garrison, B. J. *Appl. Surf. Sci.* **2004**, *231−2*, 72.

(12) Andersen, H. C. *J. Comput. Phys.* **1983**, *52*, 24.

(13) Dou, Y.; Zhigilei, L. V.; Winograd, N.; Garrison, B. J. *J. Phys. Chem. A* **2001**, *105*, 2748.

(14) Dou, Y. S.; Zhigilei, L. V.; Postawa, Z.; Winograd, N.; Garrison, B. J. *Nucl. Methods B* **2001**, *180*, 105.

(15) Brenner, D. W.; Shenderova, D. A.; Harrison, J. A.; Stuart, S. J.; Ni, B.; Sinnott, S. B. *J. Phys. D.: Condensed Matter* **2002**, *14*, 783.

(16) Berendsen, H. J. C.; Postma, J. P. M.; van Gunsteren, V. F.; Hermans, J. In *Intermolecular forces*; Pullman, B., Eds.; Reidel: Dordrecht 1981.

(17) Garrison, B. J.; Kodali, P. B. S.; Srivastava, D. *Chem. Rev.* **1996**, *96*, 1327.

(18) Kelly, R.; Miotello, A.; Mele, A.; Guidoni, A. G.; Hastie, J. W.; Schenck, P. K.; Okabe, H. *App. Surf. Sci.* **1998**, *133*, 251.

(19) NoorBatcha, I.; Lucchese, R. R. *Phys. Rev. B* **1987**, *36*, 4978.

(20) Zhigilei, L. V.; Garrison, B. J. *Rapid Commun. Mass Spectrom.* **1988**, *12*, 1273.

(21) Sunner, J.; Ikonomou, M. G.; Kebarle, P. *Int. J. Mass Spectrosc.* **1988**, *82*, 221.